Organic & Biomolecular Chemistry

This article is part of the

OBC 10th anniversary
themed issue

All articles in this issue will be gathered together online at

www.rsc.org/OBC10

Organic &
Biomolecular
Chemistry

Dynamic Article Links
View Online

Cite this: *Org. Biomol. Chem.*, 2012, **10**, 5898

www.rsc.org/obc

PAPER

Helical self-assembly and co-assembly of fluorinated, preorganized discotics†‡

Michel H. C. J. van Houtem, Faysal Benaskar, Carel F. C. Fitié, Rafael Martín-Rapún, Jef A. J. M. Vekemans and E. W. Meijer*

Received 22nd February 2012, Accepted 16th April 2012
DOI: 10.1039/c2ob25385b

The synthesis and self-assembly properties of a fluorinated C_3-symmetrical 3,3′-bis(acylamino)-2,2′-bipyridine discotic (**1**) in the mesophase and in solution are described. First, 3,4,5-tris-(1*H*,1*H*,2*H*,2*H*,3*H*,3*H*-perfluoroundecyl-1-oxy)benzoyl chloride was coupled to mono-*t*-BOC protected 2,2′-bipyridine-3,3′-diamine to afford after deprotection the corresponding fluorinated aromatic amine on a multigram scale. Then, three-fold reaction of this amine with trimesyl chloride yielded the target C_3-symmetrical fluorinated disc. The latter displayed columnar liquid crystallinity over a temperature range of more than 350 K in which helical rectangular and hexagonal columnar mesophases were detected by X-ray diffraction measurements. ^{1}H-NMR spectroscopy showed a preorganized structure due to strong intramolecular hydrogen bonding between the amide N–H's and bipyridine nitrogen atoms, even in the presence of a large excess of hexafluoroisopropanol. This preorganized structure allows the formation of helical self-assemblies in fluorinated solvents, as was established using UV-Vis spectroscopy. The fluorinated disc and two chiral hydrocarbon analogues (a C_3-symmetrical and a desymmetrized disc) were mixed in a 1 : 10 v : v mixture of methoxynonafluorobutane (MNFB) and 1,1,2-trichloro-1,2,2-trifluoroethane (Freon 113). Importantly, the C_3-symmetrical hydrocarbon disc dissolves only in the presence of fluorinated disc in the latter solvent mixture, proving a mutual interaction. CD spectroscopy performed on these mixtures points to a preference for alternating self-assemblies of fluorinated and chiral hydrocarbon discotics.

Introduction

Self-assembly of discotic molecules into well-ordered systems in solution and in the solid state is an intensively studied topic in supramolecular chemistry.[1–5] Potential applications are solar cells,[6] field-effect transistors,[7,8] nanomembranes,[9] supramolecular polymers[10] and supramolecular scaffolds for biological systems, such as bacteria.[11,12] Since the discovery of columnar liquid crystalline behaviour shown by discotics in 1977,[13] numerous disc-shaped molecules have been synthesized and investigated. Their design is based on a rigid core and a flexible aliphatic periphery which together give rise to columnar liquid crystals.[14,15] Also, this design is responsible for one-dimensional self-assemblies in solution. The control of mesophases and assemblies in solution is an important goal on the path to efficient devices and in attempting to mimic natural systems.[16–18]

Control of self-assembly of columnar mesogenic systems may rely on peripheral perfluorinated tails,[19] which stabilize mesophases,[20–26] improve alignment behavior[27] and increase phase separation.[28–31] Such improved properties have been shown for columnar self-assembling dendrons[32,33] and for dendrimers.[34–36] The self-assembly of fluorinated dendrons may induce supramolecular columnar helical liquid crystallinity with promising opto-electronic properties like high charge-carrier mobilities.[37] The latter was also achieved in columnar mesophases of partially fluorinated perylene bisimides.[38] Mesophase behaviour of hydrogen-bonded, alkylated triazines and benzoic acids has been tuned by variation of the ratio between fluorinated and hydrogenated tails.[39,40] An advantage of these intermolecularly hydrogen bonded systems is that with a limited number of precursors a wide variety of liquid crystalline materials are accessible. In solution, fluorinated porphyrin[41] and phthalocyanine[42] derivatives have been reported that possess potential gas or drug carrier applications. Fluorinated phthalocyanines possessing

---

Institute for Complex Molecular Systems and Laboratory of Organic and Macromolecular Chemistry, Eindhoven University of Technology, P. O. Box 513, 5600 MB Eindhoven, The Netherlands.
E-mail: E.W.Meijer@tue.nl

† This article is part of the *Organic & Biomolecular Chemistry* 10th Anniversary issue.

‡ Electronic supplementary information (ESI) available: TGA analysis, DSC thermogram and wide and small angle X-ray diffraction pattern of disc **1**. 1D and 2D gCOSY ^{1}H spectra of disc **1**; temperature-dependent UV-Vis absorption spectra of disc **1** in MNFB and C_9F_{20} and HFIP titration results for disc **1** in MNFB; concentration-dependent UV-Vis absorption spectra on mixtures of disc **1**–disc **3** (1 : 9 mol : mol) in **F1** : **10**; full results of Sergeant and Soldier mixing experiments on discotics **1** and **3** in **F1** : **10**. See DOI: 10.1039/c2ob25385b

catalytic activity allow recovery of the catalysts by fluorous solvent extraction.[43] Enhanced properties by introducing a fluorinated periphery may rely on the reduced miscibility of these fluorinated moieties with other parts in the molecule, the so-called fluorophobic effect.[44–46] The latter is caused by the increased rigidity, linearity and low surface energy of the perfluorinated alkyl chain compared to a hydrocarbon alkyl chain. Also, perfluorinated alkyl chains are bulkier than hydrocarbon chains, with cross sections in the 27–30 Å^2 range for the former and 18–21 Å^2 range for the latter, the exact value depending on the packing situation.[45] Fluorination of aromatic units can enhance their interaction with non-fluorinated analogues because of attractive interactions between molecules having large quadruple moments of similar magnitude but of opposite sign; this can lead to alternating assemblies.[47–51] This has been observed in the columnar mesophase for blends of triphenylene-functionalized polymers with perfluoro-triphenylenes[52] and for helical columnar aggregates.[53] Co-assemblies were observed in columnar mesophases for hexabenzocoronene–perylenebisimide mixtures,[54] symmetrical triphenylene derivatives[55,56] and mixtures of pyrene-based hydrogen bonded discotics with trinitrofluorenone as well.[57] Alternating perfluoroarene–arene interactions are also known in the organo-gel state.[58–60] As in the mesophase, co-assembly of different species in solution is usually based on donor–acceptor systems such as oligo(phenylene vinylene)s (OPVs),[61] phthalocyanines[62] and porphyrin-pyrene complexes.[63]

Our aim has been to take advantage of the fluorophobic effect to alter the self-assembly process of discotics based on the 3,3′-bis(acylamino)-2,2′-bipyridine unit. These discotics (like **2**, Fig. 1) are equipped with three trialkoxyphenyl peripheral units and are preorganized by strong intramolecular hydrogen bonding between bipyridine N atoms and amide N–H functionalities as was deduced from ^{1}H-NMR data in solution.[64] Self-assembly occurs mainly due to aromatic interactions and phase separation by which the discotics adopt a propeller conformation.[65] The latter results in a 3-fold axis of symmetry (C_3 symmetry) for discotics possessing three equivalent peripheral groups (discotic **2**, Fig. 1), thus these propeller discotics have point group C_3.[65] The propeller conformation gives rise to helical assemblies in the columnar (lyotropic) mesophase,[64–67] and in solution.[68] When decorated with polar ethylene oxide tails, helical self-assembly in polar solvents and in water is possible.[69,70] Since the helix is a chiral object, chiral information in the periphery of the discotic may be transferred to the helical stack causing a bias of the overall helical sense.[71–79] Phase separation between the rigid core and the disordered periphery of bipyridine discs depends on sufficiently long apolar hydrocarbon or polar oligo(ethylene oxide) tails and may be further enhanced by the incorporation of fluorinated tails. The latter is expected to stabilize the columnar mesophase. Accordingly, we introduce novel bipyridine discotic **1** (Fig. 1) possessing a perfluorinated periphery. The study of mixtures of discotics possessing a fluorocarbon and a hydrocarbon periphery may enable to detect novel, helical co-assemblies. Following precedent,[80–82] we sought to confirm the presence of such highly ordered, reversible helical structures in solution by the ‘Sergeant and Soldiers’ effect[83] in which a small amount of chiral discs is able to bias the helical sense of a platoon of achiral discs, the fluorinated discs in this case.

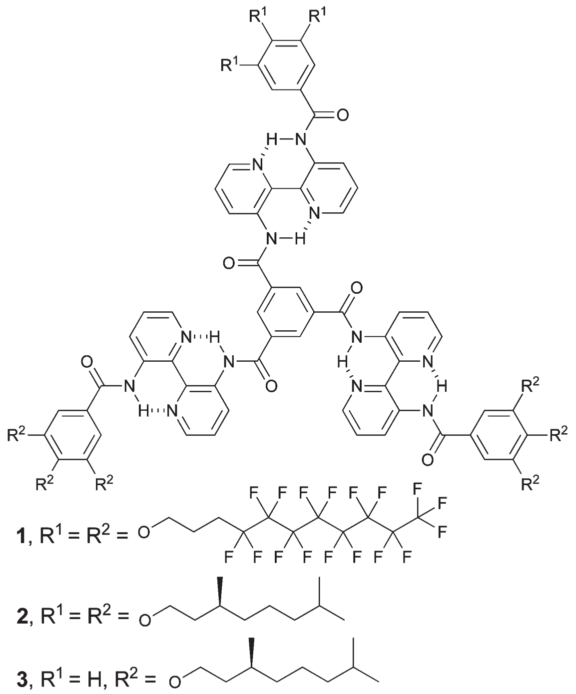

Fig. 1 Discotics presented in this study: C_3-symmetrical discs **1** and **2** equipped with nine achiral perfluoro-alkoxy and nine chiral, apolar, dihydrocitronellyloxy tails, respectively. Desymmetrized disc **3** is equipped with six dihydrocitronellyloxy tails. Intramolecular hydrogen bonding is represented with dashed bonds.

The mesophase properties of discotic **1** have been investigated using differential scanning calometry (DSC), polarizing optical microscopy (POM) and X-ray diffraction (XRD). Self-assemblies of fluorinated disc **1** and co-assemblies with chiral, hydrocarbon discotic **2** (Fig. 1) have been studied in solution using optical spectroscopy in fluorinated solvents. Also co-assemblies of fluorinated disc **1** and desymmetrized, chiral disc **3** (Fig. 1), possessing a C_1 point group when present in a propeller conformation, have been studied in solution since miscibility between discs **1** and **3** could be achieved in all ratios.

Results and discussion

Synthesis of fluorinated discotic 1

The synthesis of chiral discotics **2** and **3** was reported previously[64,68,84] and is based on a convergent approach. The synthesis of fluorinated disc **1** is based on the same considerations as those adopted in the synthesis of disc **2**. Key factors in the amide bond formation are the use of acid chlorides as electrophilic partners to compensate for the limited nucleophilicity of the aromatic amines involved, and the presence of long alkoxy tails ensuring solubility throughout synthesis and purification. The synthesis of fluorinated disc **1** is summarized in Scheme 1. First, methyl gallate (**4**) was reacted with commercially available fluorinated iodide **5** to obtain fluorinated gallic ester **6** in 85% yield by adopting a combination of literature procedures.[85–87] A hydrocarbon spacer length of at least three carbons between the aryl-oxygen and the fluorinated part is required for the

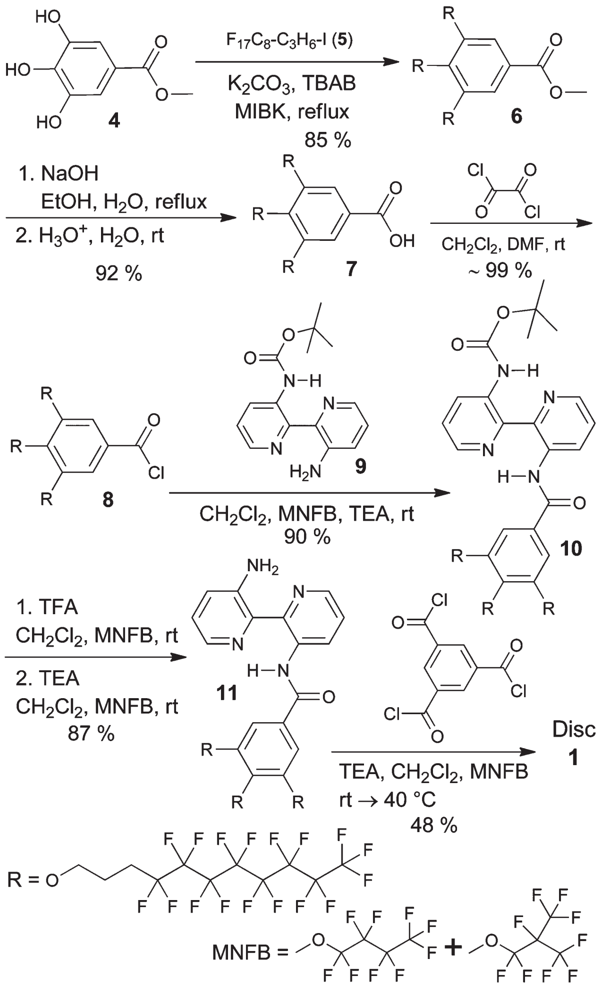

Scheme 1 Synthesis of fluorinated disc **1**. During the amidation of acid chloride **8** with amine **9** and in the subsequent reactions the use of fluorinated solvent MNFB was necessary to ensure solubility. TBAB = tetrabutylammonium bromide, MIBK = methylisobutylketone, TFA = trifluoroacetic acid, TEA = triethylamine, MNFB = methoxynonafluorobutane.

nucleophilic displacement of iodide: using a –CH_2– spacer, aromatic ether formation could not be accomplished which has been rationalized by the repulsive character of the nearby –CF_2– group[88] and employing a –C_2H_4– spacer, elimination occurred under typical Williamson ether synthesis conditions.[89,90] Fluorinated ester **6** was saponified to give carboxylic acid **7** after neutralization and this was converted into acid chloride **8**.[69] Amidation of the latter with mono-*t*-BOC protected diamine **9** afforded wedge **10** in 90% yield.[64,84,91] The solubility of the fluorinated components during reaction was ensured by employing methoxynonafluorobutane (MNFB) as a co-solvent.[92–96] Removal of the *t*-BOC group of **10** afforded mono-amine **11** after neutralization in a 88% yield. Importantly, considering multigram-scale synthesis, no column chromatographic separation was needed to purify fluorinated compounds **6**, **7**, **10** and **11**.

In the final reaction step three molar equivalents of fluorinated amine **11** were reacted with trimesyl chloride to afford target disc **1**. Purification was achieved by precipitation from mixtures of chloroform and fluorinated solvents followed by column chromatography over silica gel using a mixture of chloroform and fluorinated solvents as eluent. Hexafluoroisopropanol[97] proved to be a convenient polar component during chromatographic separation: HFIP is a good solvent for this system and HFIP suppresses aggregation of discotic **1** on the column. The purity of disc **1** was established by a combination of TLC, ^{1}H-NMR, MALDI-TOF MS and elemental analysis. The ^{1}H-NMR spectrum was assigned with the aid of gCOSY ^{1}H-^{1}H 2D NMR.[98]

Liquid crystalline properties

The mesophase properties of discotic **1** were investigated following the protocols described for hydrocarbon[64,65] and oligo(ethylene oxide) analogues.[99] Fluorinated disc **1** is a sticky compound at room temperature. The thermal stability was investigated using thermal gravimetric analysis (TGA). No loss of mass below 350 °C occurred under a nitrogen atmosphere.[100] Therefore, DSC and POM were also conducted under a nitrogen atmosphere. With DSC, a glass transition at −6 °C was observed for fluorinated disc **1**, which was confirmed by modulated DSC analysis.[101,102] The high order of the discotics in the columnar mesophase usually favours a transition to a crystal on cooling instead of a simple glass formation of the disordered side-tails.[103] Probably, the stiffness of the perfluorinated tails of discotic **1** prevents their organization into an ordered crystal.[103] Besides the glass transition, no other transitions were observed in DSC. Hence, disc **1** is liquid crystalline over a temperature window of more than 350 °C. The absence of a reachable isotropisation temperature for **1** unfortunately prevented the growth of typical textures by slow cooling. These textures are considered to be a strong proof for liquid crystallinity and provide information on the type of mesophase.[104] However, the liquid crystalline nature of discotic **1** was proven by shear alignment of a sample on a glass slide at elevated temperatures (Fig. 2). Under cross-polarizers at 200 °C, a highly birefringent sample was observed which was sensitive to pressure changes (Fig. 2a). When the sample was rotated over an angle of 45° in the cross polarizer, almost no birefringence was visible indicating alignment of the sample (Fig. 2b). The obtained textures after rubbing the sample between two glass slides (Fig. 2c) suggest the presence of a columnar mesophase.[105]

The structure of disc **1** in the mesophase was also studied by means of wide (WAXD) and small angle X-ray diffraction (SAXD). WAXD was used to study interdisc parameters and SAXD to study intercolumn parameters. Considering its molecular structure and C_3-symmetry we expected similar columnar mesophase to be present as for their hydrocarbon-tail analogues to which a helical columnar rectangular lattice was assigned.[65] Measurements were performed at 50 °C and 250 °C only, in view of the absence of any transitions in DSC above room temperature. An aligned sample provides valuable information on the helical self-assembly of the bipyridine discotics as has been shown for other helical systems.[65,67,106–114] Indeed, alignment was observed in the WAXD region.[115] Reflections belonging to a regular organization of disc **1** in its axial direction together with a diffuse diffraction belonging to disordered side-tails are a clear evidence for liquid crystalline behaviour. The results extracted from the WAXD and SAXD measurements are collected in Table 1. In WAXD at 50 °C, a halo representing a distance of 0.54 nm points to the distance between molten fluorinated alkyl tails, a distance larger than between molten hydrophobic alkyl tails (0.40–0.47 nm).[30,64,116] The difference arises from the larger rigidity of the perfluorinated tails of disc **1**, the larger C–F bond length compared to the C–H bond length and the slightly larger size of the fluor atoms compared to the hydrogen atoms with concomitant larger Van der Waals radius (1.47 Å for F and 1.20 Å for H).[45] Two reflections at 0.35 nm and 0.33 nm were observed (Table 1). The distance of 0.33 nm can be attributed to the distance between the central phenyl moieties, while the distance of 0.35 nm presumably belongs to the distance between the bipyridine centroids.[65,67] This is in correspondence with a rotation of approximately 15° of the bis(acylamino)bipyridine unit around the central phenyl moiety which is responsible for the propeller shape of disc **1** in a helical aggregate.[65,67] When the sample is heated to 250 °C, a single reflection at 0.35 nm and the halo belonging to the fluorinated alkyl tails were observed in WAXD (Table 1).[117] Apparently, at these high temperatures a columnar structure is still present but the presence of only one reflection belonging to the interdisc distance suggests that the discs adopt an on average flat conformation instead of the propeller conformation and are thus devoid of helicity.

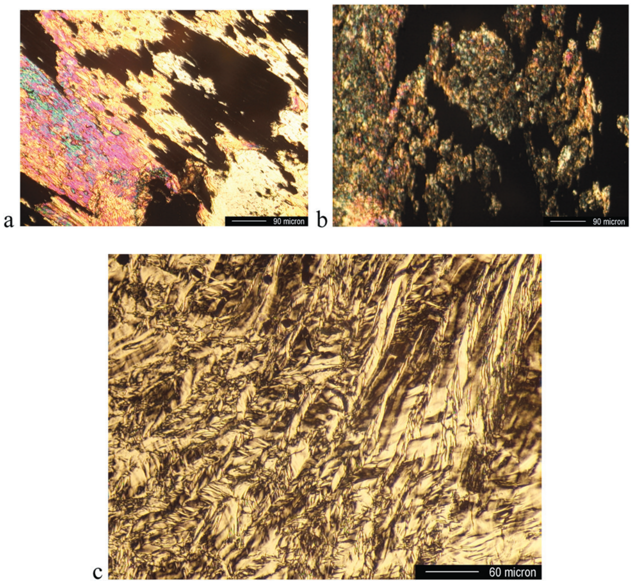

Fig. 2 POM micrographs of disc **1**. (a) Discotic **1** sheared on a glass plate at 200 °C. (b) The same sample, but rotated over 45°. (c) Textures obtained after vigorous rubbing at 160 °C.

SAXD gives information about the two-dimensional organization of disc **1** in the columnar mesophase. At 50 °C a rectangular lattice could be assigned with *p2gg* symmetry[118] according to the extinction rules (Table 1).[4] This implies that the column which is located in the centre of the rectangular unit cell differs from the others, probably due to a vertical shift between the columns.[65,67] Although no alignment was observed in the SAXD pattern,[119] a helical pitch of 76.5 Å containing 23 molecules was determined which implied a rotation of 16° between superimposed discs. This is in line with the assignment performed on its hydrocarbon analogue and desymmetrized analogues.[65,84] Probably, the larger steric demands of the perfluorinated tails cause the helical pitch of disc **1** to be smaller than that of its hydrocarbon analogue possessing nine dodecyloxy tails (pitch: 95.4 Å), but similar to that of chiral disc **2**

Table 1 XRD results for the mesophases of fluorinated disc **1** at 50 and 250 °C

T [°C]	Phase[a]	$h\ k\ l$	d_{obs} [Å]	d_{calcd} [Å]	Lattice constants [Å]
50	Col_{ro}	1 1 0	37.0	37.0	$a = 75.6$
	p2gg	0 2 0	21.3	21.3	$b = 42.5$
		2 1 1	18.5	18.6	$p = 25.5$
		3 1 1	16.4	16.3	$h = 3.3$
		2 3 0	13.1	13.3	2 molecules per unit cell
		2 3 1	11.6	11.7	$\rho_{\text{calc}} = 1.66\ \text{g cm}^{-3}$
		2 4 0	10.2	10.2	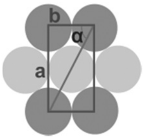
		Perfluoroalkyl	5.4		
		π–π	3.5		
		π–π	3.3		
250	Col_{ho}	1 0 0	38.5	38.5	$a = 44.5$
	p6mm	1 1 0	22.3	22.2	$h = 3.5$
		2 0 0	19.3	19.3	1 molecule per unit cell
		2 1 0	14.6	14.6	$\rho_{\text{calc.}} = 1.47\ \text{g cm}^{-3}$
		3 0 0	11.9	12.8	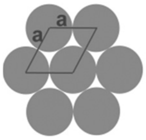
		2 2 0	11.3	11.1	
		3 1 0	10.6	10.7	
		Perfluoroalkyl	5.8 (br.)[b]		
		π–π	3.5		

[a] Col_{ro} = ordered columnar rectangular phase. Col_{ho} = ordered columnar hexagonal phase. [b] br. = broad maximum. h = interdisc distance from WAXD. p = distance along one column for a 120°-turn of the helix. $\rho_{\text{calc}}(\text{Col}_{\text{ro}}) = (10 \times Z \times M_{\text{w}})/(a \times b \times h \times 6.02)$, where M_{w} is the molecular weight and Z the number of discs per unit cell. $\rho_{\text{calc}}(\text{Col}_{\text{ho}}) = (20 \times M_{\text{w}})/(a^2 \times h \times \sqrt{3} \times 6.02)$.

possessing nine branched alkoxy tails (pitch: 76.5 Å).[65] The calculated density is in agreement with that of other reported fluorinated discotics (Table 1).[28] The mesophase at 250 °C is clearly hexagonal.[118] The structural difference between the $\mathrm{Col_{ro}}$ and $\mathrm{Col_{ho}}$ mesophases is small regarding the ratio between lattice a and b parameters of the $\mathrm{Col_{ro}}$ lattice which amounts to 1.78 $(\sim\sqrt{3})$ and the angle α which amounts to 60.6° (Table 1).[28,120–122] This small difference may explain the absence of a detectable transition in DSC between the $\mathrm{Col_{ro}}$ and $\mathrm{Col_{ho}}$ mesophases. Overall, disc **1** displays very stable columnar mesophases with a mesophase window greater than 350 K and intracolumnar order still present at elevated temperatures.

Self-assembly in solution

Self-assembly studies of highly fluorinated compounds in solution are rare due to their limited solubility in common organic solvents. One example is concentration-dependent self-assembly of hexabenzocoronenes equipped with six perfluorinated tails in trifluorotoluene.[29] Disc **1** is soluble in mixtures of methoxynonafluorobutane (MNFB), chloroform and hexafluoroisopropanol (HFIP) as well in pure MNFB, perfluorononane, trifluoroacetic acid and hexafluorobenzene. ^{1}H-NMR spectroscopy is a convenient tool to show the presence of intramolecular hydrogen bonding and preorganization in bipyridine discotics which is responsible for the appealing self-assembly properties.[64,84] Discotic **1** was dissolved in a mixture of 20 vol% HFIP in $\mathrm{CDCl_3}$[123] and a 1 : 1 v : v mixture of HFIP–HFIP-$\mathrm{D_2}$ was used to ensure the visibility of the exchangeable amide N–H hydrogens (Fig. 3a). The downfield shifted hydrogens **a** and **b** point to strong intramolecular hydrogen bonding of the amide N–H with the bipyridine nitrogens which is remarkable in the presence of HFIP, being a strong hydrogen bond breaking solvent. Hydrogens **a** and **b** are split while their integral value is approx. 50% of the integral value for the other hydrogens, indicating that partial H–D exchange has taken place (Fig. 3b). The weaker acidity of an amide N–D compared to an amide N–H will result in a weaker intramolecular hydrogen bond of the former which affects the other amide N–H and induces a little upfield shift.[126] Bipyridine hydrogens **c** and **e** are positioned downfield (9.2 and 9.0 ppm, respectively) as a result of anisotropic deshielding by the nearby amide carbonyls indicating the in-plane conformation of the amide and bipyridine moieties. Bipyridine hydrogen **f** is shifted significantly more downfield than similar hydrogen **g** (8.6 ppm *versus* 8.4 ppm) due to a deshielding influence of the amide carbonyl of the neighbouring wedge. This indicates an on average planar conformation of the whole compound, which is important to enable columnar stacking.

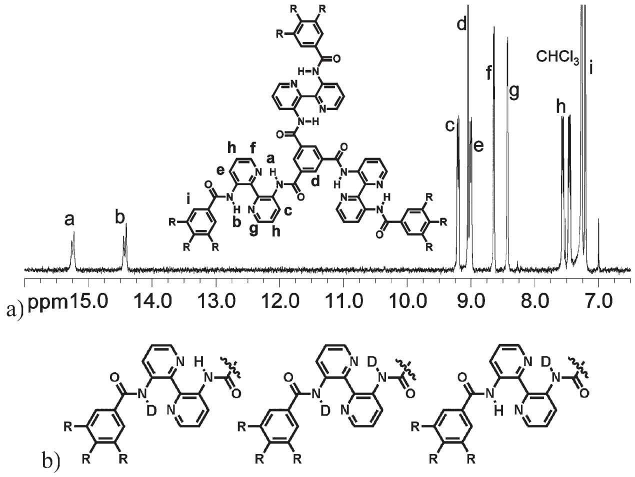

Fig. 3 (a) ^{1}H-NMR spectrum of discotic **1** in HFIP–HFIP-$\mathrm{D_2}$–$\mathrm{CDCl_3}$ (20 vol% HFIP–HFIP-$\mathrm{D_2}$ (1 : 1) in $\mathrm{CDCl_3}$, 3.8 mM).[124] Only the aromatic and hydrogen bonding regions are shown.[125] R = $\mathrm{OC_3H_6C_8F_{17}}$. (b) The three possible deuterated states of a 3,3′-(bisacylamino)-2,2′-bipyridyl wedge.

Self-assembly of discotic **1** in perfluorononane[127] (Fig. 4a) and MNFB (Fig. 4b) has been studied by UV-Vis spectroscopy.[68–70,128,129]

Four distinct absorption maxima were observed of which the typical splitting pattern with maxima at 362 nm and 381 nm and the shoulder at 346 nm originate from the diamino bipyridine chromophore (Fig. 4).[68,131] This typical splitting pattern was attributed to the presence of well-organized helical assemblies of discotic **1** in perfluorononane or MNFB.[68] When the temperature was increased from 15 °C to 115 °C and 55 °C, respectively,[132] almost no changes in the UV-Vis spectra were observed, suggesting that the assemblies of disc **1** are stable in these solvents even at a concentration of 5 μM. This contrasts with solutions of hydrocarbon-tail discs like disc **2** in dodecane in which a blue shift together with a hyperchromic shift indicate melting of the helical assemblies upon heating to 110 °C.[68] The molecularly dissolved state of disc **1** was reached, however, by addition of a highly competitive solvent for stacking like HFIP or TFA (Fig. 5a).

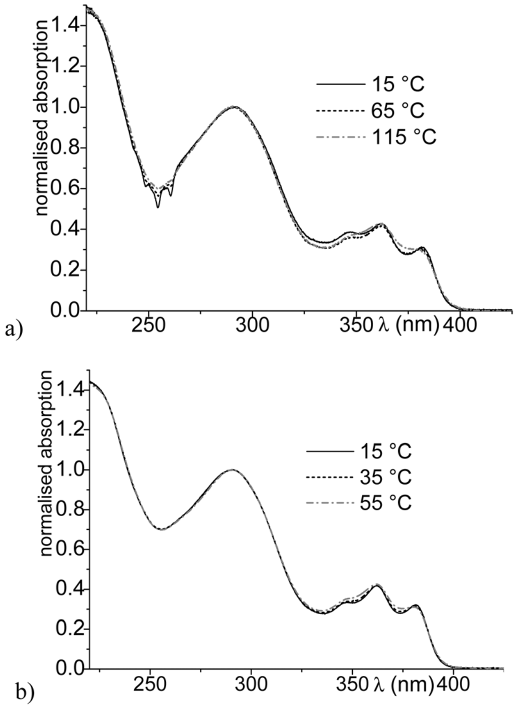

Fig. 4 UV-Vis absorption spectra of discotic **1** in (a) $\mathrm{C_9F_{20}}$ (5.5 μM), (b) MNFB (5.7 μM) at three temperatures. Spectra are normalized to the absorption maximum at 292 nm.[130]

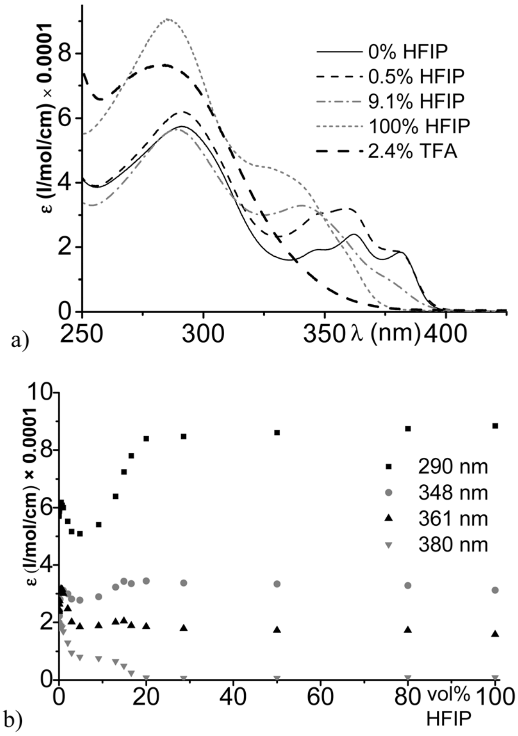

Fig. 5 (a) UV data from addition of a 17 μM solution of disc **1** in HFIP to a 17 μM solution of disc **1** in MNFB. Amounts of HFIP and TFA refer to volume-%.[133] (b) Course of the extinction coefficients corresponding to the absorption maxima displayed by disc **1** in pure MNFB.[134]

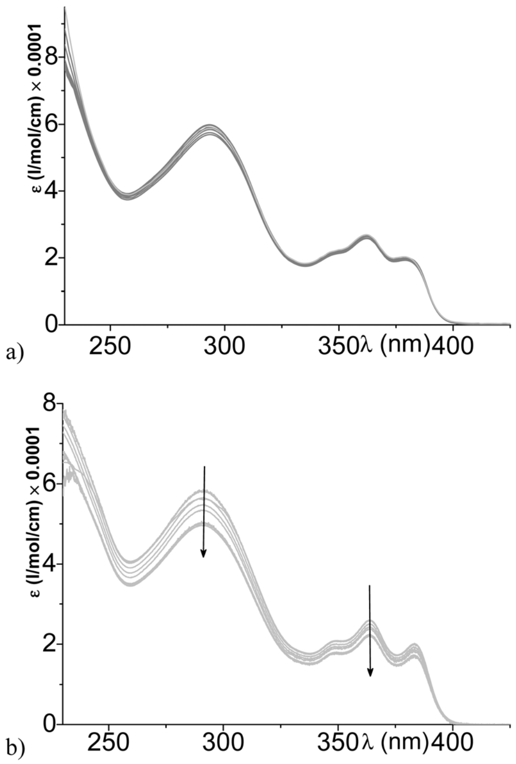

Fig. 6 Concentration-dependent UV-Vis absorption spectra of (a) disc **1** between 0.30 and 0.0056 mM and (b) disc **3** between 0.50 and 0.0010 mM. The arrows indicate the change upon lowering the concentration. Spectra obtained in MNFB : Freon113 1 : 10 v : v (**F1 : 10**).[135]

A large hyperchromic effect and fading of the typical splitting pattern in the bipyridine chromophore region was observed at increased HFIP fraction (Fig. 5a). Surprisingly, even at 0.5 vol% of HFIP rupture of the helical self-assembly of disc **1** was observed as is illustrated by the large difference of the curves corresponding to 0 vol% and 0.5 vol% HFIP. The latter curve resembles the absorption spectrum of hydrocarbon discotics in the molecularly dissolved state.[68] With increased HFIP fraction, these absorptions merge into a broad shoulder around 330 nm. The change in absorption levels off after addition of 20 vol% of HFIP (Fig. 5b) indicating that only the molecularly dissolved state is present above 20 vol% HFIP. The addition of a small amount of TFA erases the absorption bands belonging to the intramolecular hydrogen-bonded bipyridine moiety due to pyridine-N protonation (Fig. 5a, black, dashed line) thus erasing the preorganized structure of disc **1**. Summarizing, disc **1** forms helical self-assemblies with equal amounts of left and right handed helices in fluorinated alkane solvents which can be disrupted by the addition of highly competitive solvents like HFIP.

Amplification of chirality and co-assembly of fluorinated and non-fluorinated discotics in solution

To gain mixed assemblies, fluorinated achiral disc **1** was mixed with chiral hydrocarbon discs **2** or **3** in a solvent in which both discs are soluble and helically aggregated. This solvent appeared to be a 1 : 10 v : v mixture of methoxynonafluorobutane and 1,1,2-trichloro-1,2,2-trifluoroethane (Freon 113), abbreviated as **F1 : 10**. The maximal concentration of fluorinated disc **1** and desymmetrized disc **3** in **F1 : 10** is 0.25 mM and 0.75 mM, respectively. Changing the 1 : 10 v : v ratio of the solvent mixture rendered either disc **1** or disc **3** insoluble. Surprisingly, C_3-symmetrical chiral disc **2** was insoluble in this solvent mixture, even at micromolar concentrations. However, disc **2** can be dissolved upon addition of at least 10 mol% of fluorinated disc **1** until a concentration of about 0.4 mM, which provides strong evidence for the presence of both fluorinated disc **1** and apolar disc **2** in the same aggregate. Concentration dependent UV-Vis spectroscopic measurements have been performed to investigate the stability of self-assemblies in **F1 : 10** (Fig. 6).

Discs **1**, **2**, and **3** are helically aggregated in **F1 : 10**, as indicated by the split absorption pattern around 350 nm (Fig. 6).[68] The extinction coefficients of disc **1** are independent of the concentration; implying that fluorinated disc **1** is probably completely aggregated at all measured concentrations (Fig. 6a). Disc **3**, however, displays a little concentration dependency; indicating incomplete aggregation at lower concentrations (Fig. 6b). The 1 : 9 molar mixture of C_3-symmetrical discs **1** and **2** barely display concentration dependence.[136]

Mixtures of fluorinated disc **1** and chiral disc **3** were made by mixing equimolar solutions of the pure components in **F1 : 10** and subsequent annealing by fast heating to 45 °C followed by cooling.[137,138] Mixing experiments were performed at several compositions with a total disc concentration of 15 μM, for which the CD and UV-Vis spectra are shown in Fig. 7.

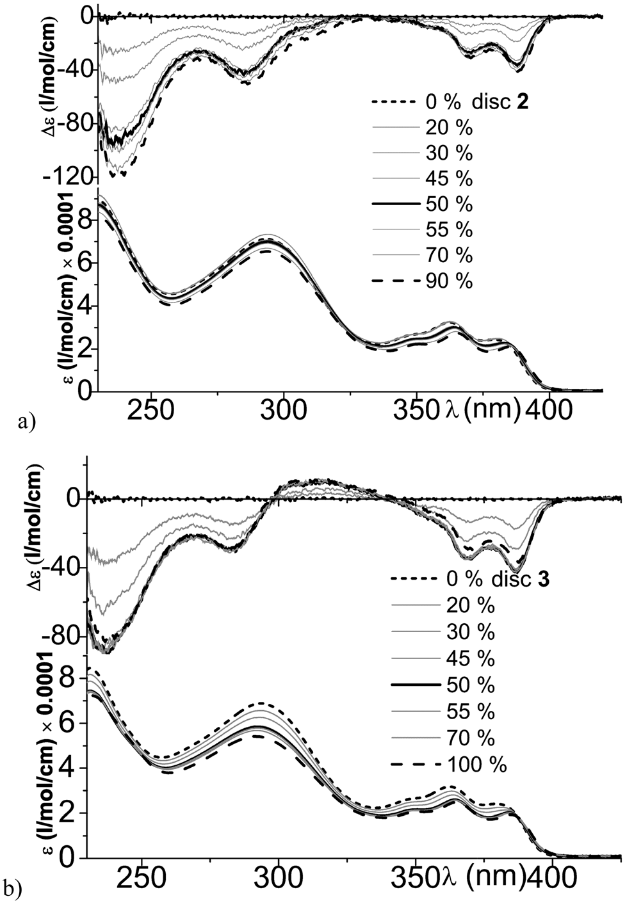

Fig. 7 CD and UV-Vis spectra deduced from the mixing experiments. (a) Mixing of a solution of chiral disc **2** containing 10 mol% disc **1** with a solution of fluorinated disc **1**. (b) Mixing of a solution of chiral disc **3** with a solution of fluorinated disc **1**. Total concentration = 15 µM, solvent: **F1** : **10**.

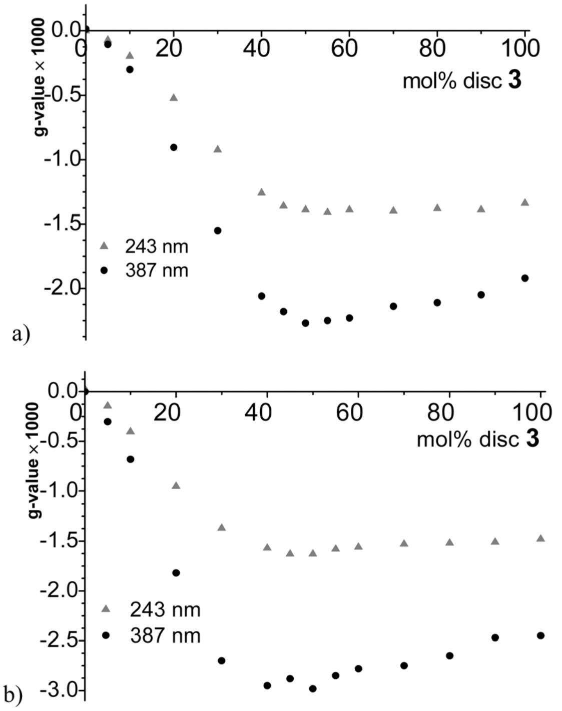

Fig. 8 Mixing experiments with equimolar solutions of discs **1** and **3**. (a) Total concentration = 15 µM and (b) Total concentration = 100 µM. Measurements performed a 1 cm and 1 mm quartz cuvette, respectively. Solvent: **F1** : **10**. *g*-Values displayed as function of the amount of chiral disc **3** present at two representative wavelengths corresponding to two maxima in the CD spectra.[140]

Both the mixtures of disc **1** with disc **2** and disc **1** with disc **3** demonstrate Cotton effects in CD spectroscopy, indicating helices of biased sense (Fig. 7). As expected, an increase of the CD effect with increasing amount of chiral disc was observed. Surprisingly, after addition of 50 mol% chiral disc, the Cotton effect did not increase further but slightly diminished, which can be rationalized by a more efficient packing of achiral discs **1** compared to that of chiral discs **3** possessing branched side tails. Apparently, the bias of helical sense of the assemblies of discs **1** and **2** or **3** is maximal after addition of 50 mol% chiral disc. The absolute value of the Cotton effect (app. −45 M^{-1} cm^{-1} at 387 nm) corresponds to values observed for pure chiral discs in apolar solution;[65,68,84] probably all helices are biased at this point. The absorption spectra depicted in Fig. 7 point to the presence of a similar type of helices during the mixing experiments, although a small decrease of the extinction coefficient was observed, especially in Fig. 7b, together with a red shift.[139] In Fig. 8 and 9 the dimensionless g-factors as function of the amount of chiral disc present at 15 µM and 100 µM or 150 µM total disc concentration are shown.

The non-linear relationship between the observed CD effect and the amount of chiral disc **3** in the solutions shown in Fig. 8a and b are a clear evidence for transfer of chirality from chiral discs **3** to achiral discs **1** in one type of aggregate.[68] The maximal Cotton effect reached at about 50 molar% chiral disc **3** is in agreement with an amplification of chirality (*i.e.* the *g*-value) by a factor two. This, together with an almost linear increase of the CD effect depicted in the first half of the mixing curve and the subsequent rather sharp transition, can be interpreted as a preference for alternating assembly of chiral disc **3** and fluor disc **1**. Such preference for alternating self-assembly was observed for mesogenic alkyl 4-[2-(perfluoroalkyl)ethoxy]-benzoates which show a favourable interaction between hydrocarbon and fluorocarbon tails depending on the length of the alkyl tail.[142,143] The results from the mixing of chiral disc **2** with fluorinated disc **1** (Fig. 9) are similar to the results displayed in Fig. 8 although the transition at 40–60 molar% chiral disc is less pronounced. The measuring point of 100 mol% chiral disc **2** cannot be reached due to the insolubility of disc **2** in **F1** : **10** in the absence of fluorinated disc **1**. Evidence of increased stack stability for mixed solutions of discotics **1** with **3** and **1** with **2**, respectively, was gained from fluorescence spectra (Fig. 10).

Discotics **1**, **2**, and **3** and their previously reported analogues are known to luminesce around 513 nm after excitation when they are present in the self-assembled helical state. The fluorescence is strongly quenched upon melting of the helical aggregates and this coincides with a blue shift in UV-Vis.[131,144]

From Fig. 10, it can be deduced that the solutions of disc **1** (black dashed line) and the 50 : 50 mixtures of discs **1** and **2** (black line) or **3** (light-grey line) display higher fluorescence

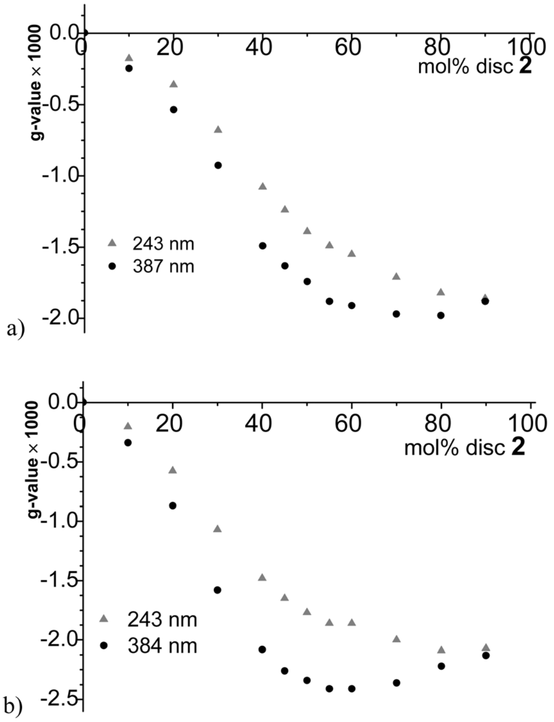

Fig. 9 Mixing experiments with a solution of disc **1** with a solution of C_3-symmetrical disc **2** containing 10 mol% disc **1**. (a) Total concentration = 15 μM and (b) Total concentration = 150 μM. Measurements performed in a 1 cm and a 1 mm quartz cuvette, respectively. Solvent: **F1** : **10**. *g*-Values displayed at two representative wavelengths corresponding to two maxima in the CD spectra.[141]

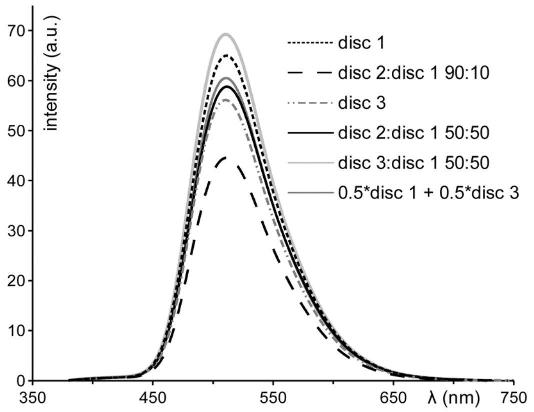

Fig. 10 Fluorescence spectra of discs **1**, **2** (in the presence of 10 mol% disc **1**) and **3** and their 1 : 1 mixtures in **F1** : **10**. Measurements performed in a 1 cm quartz cuvette, conc. = 1 μM, excitation at 365 nm. Graphs were normalized to the absorption of the mixtures at 365 nm (absorption data obtained from Fig. 6 and 7). The dark-grey line (0.5*disc **1** + 0.5*disc **3**) is obtained by addition of the graphs belonging to pure discs **1** and **3** (*i.e.* the black and grey dashed graphs) and division by two.

intensities compared to solutions of chiral discs **3** (dark-grey dashed line) and **2** (in the presence of 10 mol% disc **1**) (large-dashed black line). This is in agreement with the concentration-dependent UV-Vis absorption results from Fig. 6: discs **2** and **3** are probably less aggregated compared to fluorinated disc **1** and the 1 : 1 mixtures. This implies that the mixed aggregate is more stable compared to chiral discs **2** and **3** alone and that the formation of the former is preferred over phase separation into aggregates composed of only disc **1** and only of discs **3** or **2**.[145] The latter is confirmed by calculating the fluorescence of the corresponding 50 : 50 mixture (dark-grey line) from data of the pure solutions, which suggests being smaller than observed in reality (Fig. 10). Finally, the preference for alternating assembly between the fluoro- and hydrocarbon discs is represented schematically in Fig. 11. In real time, there will be a dynamic equilibrium between these alternating and pure assemblies. When an excess of fluorinated disc **1** was applied (*i.e.* less than 50 mol% chiral disc), alternating aggregates (assembly A, Fig. 11) and pure achiral, fluorinated columns (assembly B, Fig. 11) may be present, the latter consisting of an equal amount of left- and right-handed helices. An excess of chiral discs **2** or **3** may result in the presence of only alternating and pure chiral, hydrocarbon columns (assembly A, Fig. 11). Thus, in the two latter cases in Fig. 11, only helices of one handedness are present rationalizing the more or less horizontal course of the curves above 50 molar % chiral disc in Fig. 8 and 9.

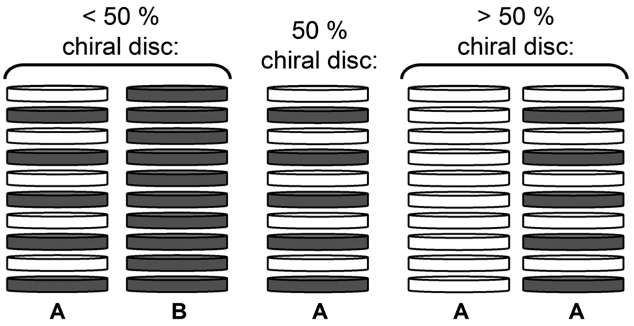

Fig. 11 Simplified representation of the types of helical assemblies of discs **1** and **2** or **3** present in the mixtures in **F1** : **10**. Dark disc≡fluor disc **1**, light disc≡chiral disc **2** or **3**. A = helices of biased sense, B = non-biased helices.

Conclusions

Novel C_3-symmetrical 3,3′-bis(acylamino)-2,2′-bipyridine discotic **1** possessing three peripheral fluorinated 3,4,5-trialkoxyphenyl wedges demonstrated to afford stable self-assemblies in the mesophase and in solution and allows the formation of mixed helical self-assemblies with hydrocarbon discotics in fluorinated solvents. These appealing properties are caused by the presence of nine peripheral heptadecafluoroundecanyloxy tails which allows the 'fluorophobic effect', *i.e.* strong phase separation between the disc's aromatic core and the fluorinated aliphatic periphery to occur. A fluorinated wedge was synthesized on a multigram scale in good yield and was converted into the desired fluorinated disc **1** but may also serve as a building block for desymmetrized discotics possessing a single fluorinated wedge with intriguing phase separation behaviour. Fluorinated disc **1** displays very stable columnar mesophase behaviour. X-ray diffraction revealed a low temperature helical rectangular columnar and a high temperature hexagonal columnar mesophase for disc **1**. However, DSC revealed only a glass transition at −6 °C, suggesting that the transition between the two columnar mesophases is gradual and of small energy difference. Helical organization originates from the self-assembly of propeller-shaped discotics, enabled by a six-fold strong intramolecular hydrogen bonding within the aromatic amide core. Temperature-stable helical self-assemblies of disc **1** were detected in fluorinated solvents which could be disrupted by the addition of competitive solvents. Fluorinated disc **1** and chiral hydrocarbon discs **2** or **3** are miscible in a mixture of methoxynonafluorobutane and 1,1,2-trichloro-1,2,2-trifluoroethane. Surprisingly, C_3-symmetrical disc **2** dissolved *only* in the presence of fluorinated disc **1** suggesting a mutual interaction between these discs in solution. Further mixing experiments of fluorinated disc **1** with chiral discs **2** and **3** revealed amplification of chirality *via* the 'Sergeant and Soldiers effect' by a factor of two. The rather linear increase of the Cotton effect up to 50 mol% chiral disc indicates the preference for alternating chiral and fluorinated discs. This is an unprecedented phenomenon in supramolecular interactions between discotics with fluorocarbon and hydrocarbon tails, respectively.

Acknowledgements

We thank Dr Xianwen Lou and Ralf Bovee for performing the MALDI-TOF MS measurements and Henk Eding for performing elemental analysis. Ben Norder and Dr Eduardo Mendes of the Technical University of Delft are acknowledged for providing access to their X-ray diffraction setup. This work was financially supported by the NRSC-Catalysis institute. R.M.-R. acknowledges support from an EU Marie Curie Intra-European Fellowship (project MEIF-CT-2006-042044) within the EC Sixth Framework Programme.

Notes and references

1 L. Brunsveld, B. J. B. Folmer, E. W. Meijer and R. P. Sijbesma, *Chem. Rev.*, 2001, **101**, 4071–4097.
2 R. J. Bushby and O. R. Lozman, *Curr. Opin. Colloid Interface Sci.*, 2002, **7**, 343–354.
3 S. Kumar, *Chem. Soc. Rev.*, 2006, **35**, 83–109.
4 S. Laschat, A. Baro, N. Steinke, F. Giesselmann, C. Hägele, G. Scalia, R. Judele, E. Kapatsina, S. Sauer, A. Schreivogel and M. Tosoni, *Angew. Chem., Int. Ed.*, 2007, **46**, 4832–4887.
5 S. Sergeyev, W. Pisula and Y. H. Geerts, *Chem. Soc. Rev.*, 2007, **36**, 1902–1929.
6 L. Schmidt-Mende, A. Fechtenkotter, K. Müllen, E. Moons, R. H. Friend and J. D. MacKenzie, *Science*, 2001, **293**, 1119–1122.
7 I. O. Shklyarevskiy, P. Jonkheijm, N. Stutzmann, D. Wasserberg, H. J. Wondergem, P. C. M. Christianen, A. P. H. J. Schenning, D. M. De Leeuw, Ž. Tomović, J. Wu, K. Müllen and J. C. Maan, *J. Am. Chem. Soc.*, 2005, **127**, 16233–16237.
8 Y. Kikuzawa, T. Mori and H. Takeuchi, *Org. Lett.*, 2007, **9**, 4817–4820.
9 C. F. C. Fitié, I. Tomatsu, D. Byelov, W. H. de Jeu and R. P. Sijbesma, *Chem. Mater.*, 2008, **20**, 2394–2404.
10 J. Roosma, T. Mes, P. Leclère, A. R. A. Palmans and E. W. Meijer, *J. Am. Chem. Soc.*, 2008, **130**, 1120–1121.
11 M. K. Müller and L. Brunsveld, *Angew. Chem., Int. Ed.*, 2009, **48**, 2921–2924.
12 M. K. Müller, K. Petkau and L. Brunsveld, *Chem. Commun.*, 2011, **47**, 310–312.
13 S. Chandrasekhar, B. K. Sadashiva and K. A. Suresh, *Pramana*, 1977, **9**, 471–480.
14 S. Chandrasekhar and G. S. Ranganath, *Rep. Prog. Phys.*, 1990, **53**, 57–84.
15 D. Demus, J. Goodby, G. W. Gray, H. W. Spiess, V. Vill, W. G. John and W. G. George, *Handbook of Liquid Crystals*, 2008, vol. 1, p. 17–23.
16 D. N. Reinhoudt and M. Crego-Calama, *Science*, 2002, **295**, 2403–2407.
17 T. Kato, *Science*, 2002, **295**, 2414–2418.
18 R. F. Service, *Science*, 2002, **295**, 2398–2399.
19 Fluorinated calamitic liquid crystals display improved mesophase properties as well as remarkable physical properties (see ref. 44).
20 U. Dahn, C. Erdelen, H. Ringsdorf, R. Festag, J. H. Wendorff, P. A. Heiney and N. C. Maliszewskyj, *Liq. Cryst.*, 1995, **19**, 759–764.
21 A. Pegenau, H. C. Xiao, C. Tschierske, P. Goring and S. Diele, *New J. Chem.*, 1999, **23**, 465–467.
22 N. Terasawa, H. Monobe, K. Kiyohara and Y. Shimizu, *Chem. Lett.*, 2003, **32**, 214–215.
23 R. Soler, E. Badetti, M. Moreno-Manas, A. Vallribera, R. M. Sebastian, F. Vera, J. L. Serrano and T. Sierra, *Liq. Cryst.*, 2007, **34**, 235–240.
24 Y. Sasada, H. Monobe, Y. Ueda and Y. Shimizu, *Chem. Commun.*, 2008, 1452–1454.
25 G. Yang, K. Zhao, W. Yu, P. Hu and B. Wang, *Sci. China, Ser. B: Chem.*, 2009, **52**, 1244–1252.
26 H.-M. Chen, K.-Q. Zhao, L. Wang, P. Hu and B.-Q. Wang, *Soft Mater.*, 2011, **9**, 359–381.
27 X. Zhou, S.-W. Kang, S. Kumar and Q. Li, *Liq. Cryst.*, 2009, **36**, 269–274.
28 B. Alameddine, O. F. Aebischer, W. Amrein, B. Donnio, R. Deschenaux, D. Guillon, C. Savary, D. Scanu, O. Scheidegger and T. A. Jenny, *Chem. Mater.*, 2005, **17**, 4798–4807.
29 O. F. Aebischer, A. Aebischer, P. Tondo, B. Alameddine, M. Dadras, H. U. Gudel and T. A. Jenny, *Chem. Commun.*, 2006, 4221–4223.
30 O. F. Aebischer, A. Aebischer, B. Donnio, B. Alameddine, M. Dadras, H. U. Gudel, D. Guillon and T. A. Jenny, *J. Mater. Chem.*, 2007, **17**, 1262–1267.
31 O. F. Aebischer, D. T. Muñoz, P. Tondo, J.-L. Débieux and T. A. Jenny, *Synthesis*, 2010, 1123–1140.
32 G. Johansson, V. Percec, G. Ungar and J. P. Zhou, *Macromolecules*, 1996, **29**, 646–660.
33 V. Percec, G. Johansson, G. Ungar and J. Zhou, *J. Am. Chem. Soc.*, 1996, **118**, 9855–9866.
34 K. Lorenz, H. Frey, B. Stuhn and R. Mülhaupt, *Macromolecules*, 1997, **30**, 6860–6868.
35 R. Martín-Rapún, M. Marcos, A. Omenat, J. L. Serrano, E. T. de Givenchy and F. Guittard, *Liq. Cryst.*, 2007, **34**, 395–400.
36 S. Hernández-Ainsa, J. Barberá, M. Marcos and J. L. Serrano, *Chem. Mater.*, 2010, **22**, 4762–4768.
37 V. Percec, M. Glodde, T. K. Bera, Y. Miura, I. Shiyanovskaya, K. D. Singer, V. S. K. Balagurusamy, P. A. Heiney, I. Schnell, A. Rapp, H. W. Spiess, S. D. Hudson and H. Duan, *Nature*, 2002, **419**, 384–387.
38 Z. An, J. Yu, B. Domercq, S. C. Jones, S. Barlow, B. Kippelen and S. R. Marder, *J. Mater. Chem.*, 2009, **19**, 6688–6698.
39 D. Janietz and A. Kohlmeier, *Liq. Cryst.*, 2009, **36**, 685–703.
40 A. Kohlmeier and D. Janietz, *Chem.–Eur. J.*, 2010, **16**, 10453–10461.
41 T. Bíza, R. Kaplánek, M. Havlík, B. Dolenský, Z. Kejík, P. Martásek and V. Král, *Supramol. Chem.*, 2008, **20**, 237–242.
42 M. Özer, A. Altındal, A. R. Özkaya and Ö. Bekaroğlu, *Dalton Trans.*, 2009, 3175–3181.
43 M. Özer, F. Yılmaz, H. Erer, I. Kani and Ö. Bekaroğlu, *Appl. Organomet. Chem.*, 2009, **23**, 55–61.
44 M. Hird, *Chem. Soc. Rev.*, 2007, **36**, 2070–2095.
45 M. P. Krafft and J. G. Riess, *Chem. Rev.*, 2009, **109**, 1714–1792.
46 V. H. Dalvi and P. J. Rossky, *Proc. Natl. Acad. Sci. U. S. A.*, 2010, **107**, 13603–13607.
47 C. R. Patrick and G. S. Prosser, *Nature*, 1960, **187**, 1021–1021.
48 T. Dahl, *Acta Chem. Scand., Ser. A*, 1988, **42**, 1–7.
49 G. W. Coates, A. R. Dunn, L. M. Henling, D. A. Dougherty and R. H. Grubbs, *Angew. Chem., Int. Ed. Engl.*, 1997, **36**, 248–251.
50 C. A. Hunter, K. R. Lawson, J. Perkins and C. J. Urch, *J. Chem. Soc., Perkin Trans. 2*, 2001, 651–669.
51 K. Reichenbacher, H. I. Suss and J. Hulliger, *Chem. Soc. Rev.*, 2005, **34**, 22–30.
52 M. Weck, A. R. Dunn, K. Matsumoto, G. W. Coates, E. B. Lobkovsky and R. H. Grubbs, *Angew. Chem., Int. Ed.*, 1999, **38**, 2741–2745.
53 K. Kishikawa, K. Oda, S. Aikyo and S. Kohmoto, *Angew. Chem., Int. Ed.*, 2007, **46**, 764–768.

54 W. Pisula, M. Kastler, D. Wasserfallen, J. W. F. Robertson, F. Nolde, C. Kohl and K. Müllen, *Angew. Chem., Int. Ed.*, 2006, **45**, 819–823.
55 O. A. Ekaterina, B. Neville, J. B. Richard, R. L. Owen, G. V. Jeremy and W. Andrew, *Angew. Chem., Int. Ed.*, 2000, **39**, 2333–2336.
56 R. J. Bushby, J. Fisher, O. R. Lozman, S. Lange, J. E. Lydon and S. R. McLaren, *Liq. Cryst.*, 2006, **33**, 653–664.
57 Y. Kamikawa and T. Kato, *Org. Lett.*, 2006, **8**, 2463–2466.
58 A. F. M. Kilbinger and R. H. Grubbs, *Angew. Chem., Int. Ed.*, 2002, **41**, 1563–1566.
59 S. S. Babu, V. K. Praveen, S. Prasanthkumar and A. Ajayaghosh, *Chem.–Eur. J.*, 2008, **14**, 9577–9584.
60 B.-K. An, D.-S. Lee, J.-S. Lee, Y.-S. Park, H.-S. Song and S. Y. Park, *J. Am. Chem. Soc.*, 2004, **126**, 10232–10233.
61 F. J. M. Hoeben, L. M. Herz, C. Daniel, P. Jonkheijm, A. P. H. J. Schenning, C. Silva, S. C. J. Meskers, D. Beljonne, R. T. Phillips, R. H. Friend and E. W. Meijer, *Angew. Chem., Int. Ed.*, 2004, **43**, 1976–1979.
62 A. de la Escosura, M. V. Martínez-Díaz, P. Thordarson, A. E. Rowan, R. J. M. Nolte and T. Torres, *J. Am. Chem. Soc.*, 2003, **125**, 12300–12308.
63 T. Sagawa, S. Fukugawa, T. Yamada and H. Ihara, *Langmuir*, 2002, **18**, 7223–7228.
64 A. R. A. Palmans, J. A. J. M. Vekemans, H. Fischer, R. A. Hikmet and E. W. Meijer, *Chem.–Eur. J.*, 1997, **3**, 300–307.
65 T. Metzroth, A. Hoffmann, R. Martín-Rapún, M. M. J. Smulders, K. Pieterse, A. R. A. Palmans, J. A. J. M. Vekemans, E. W. Meijer, H. W. Spiess and J. Gauss, *Chem. Sci.*, 2011, **2**, 69–76.
66 A. R. A. Palmans, J. A. J. M. Vekemans, R. A. Hikmet, H. Fischer and E. W. Meijer, *Adv. Mater.*, 1998, **10**, 873–876.
67 R. Martín-Rapún, D. Byelov, A. R. A. Palmans, W. H. de Jeu and E. W. Meijer, *Langmuir*, 2009, **25**, 8794–8801.
68 A. R. A. Palmans, J. A. J. M. Vekemans, E. E. Havinga and E. W. Meijer, *Angew. Chem., Int. Ed. Engl.*, 1997, **36**, 2648–2651.
69 L. Brunsveld, H. Zhang, M. Glasbeek, J. A. J. M. Vekemans and E. W. Meijer, *J. Am. Chem. Soc.*, 2000, **122**, 6175–6182.
70 L. Brunsveld, B. G. G. Lohmeijer, J. A. J. M. Vekemans and E. W. Meijer, *Chem. Commun.*, 2000, 2305–2306.
71 J. Malthête, J. Jacques, N. H. Tinh and C. Destrade, *Nature*, 1982, **298**, 46–48.
72 K. Yamamura, S. Ono, H. Ogoshi, H. Masuda and Y. Kuroda, *Synlett*, 1989, 18–19.
73 M. M. Green, H. Ringsdorf, J. Wagner and R. Wüstefeld, *Angew. Chem., Int. Ed. Engl.*, 1990, **29**, 1478–1481.
74 C. F. van Nostrum, A. W. Bosman, G. H. Gelinck, S. J. Picken, P. G. Schouten, J. M. Warman, A. J. Schouten and R. J. M. Nolte, *J. Chem. Soc., Chem. Commun.*, 1993, 1120–1122.
75 I. Danila, F. Riobé, F. Piron, J. Puigmartí-Luis, J. D. Wallis, M. Linares, H. Ågren, D. Beljonne, D. B. Amabilino and N. Avarvari, *J. Am. Chem. Soc.*, 2011, **133**, 8344–8353.
76 Helical self-assembly has been observed in the mesophase and in solution for other supramolecular systems as well, see ref. 77–80 for some relevant reviews.
77 D. B. Amabilino and J. Veciana, *Supramol. Chem.*, 2006, **265**, 253–302.
78 G. Gottarelli, S. Lena, S. Masiero, S. Pieraccini and G. P. Spada, *Chirality*, 2008, **20**, 471–485.
79 F. Vera, J. L. Serrano and T. Sierra, *Chem. Soc. Rev.*, 2009, **38**, 781–796.
80 A. R. A. Palmans and E. W. Meijer, *Angew. Chem., Int. Ed.*, 2007, **46**, 8948–8968.
81 A. Lohr and F. Würthner, *Chem. Commun.*, 2008, 2227–2229.
82 T. Yamamoto, T. Fukushima, A. Kosaka, W. Jin, Y. Yamamoto, N. Ishii and T. Aida, *Angew. Chem., Int. Ed.*, 2008, **47**, 1672–1675.
83 M. M. Green, M. P. Reidy, R. D. Johnson, G. Darling, D. J. O'Leary and G. Willson, *J. Am. Chem. Soc.*, 1989, **111**, 6452–6454.
84 M. H. C. J. van Houtem, R. Martín-Rapún, J. A. J. M. Vekemans and E. W. Meijer, *Chem.–Eur. J.*, 2010, **16**, 2258–2271.
85 M. C. Hersmis, A. J. H. Spiering, R. J. M. Waterval, J. Meuldijk, J. A. J. M. Vekemans and L. A. Hulshof, *Org. Process Res. Dev.*, 2001, **5**, 54–60.
86 A. P. Narrainen, L. R. Hutchings, I. Ansari, R. L. Thompson and N. Clarke, *Macromolecules*, 2007, **40**, 1969–1980.
87 R. Kaplánek, M. Havlík, V. Král, P. Martásek and T. Bříza, *Synth. Commun.*, 2010, **40**, 247–256.
88 D. O'Hagan, *Chem. Soc. Rev.*, 2008, **37**, 308–319.
89 C. S. Rondestvedt and G. L. Thayer, *J. Org. Chem.*, 1977, **42**, 2680–2683.
90 N. O. Brace, L. W. Marshall, C. J. Pinson and G. Vanwingerden, *J. Org. Chem.*, 1984, **49**, 2361–2368.
91 Mono-amidated 2,2′-bipyridine-3,3′-diamine can be obtained by selective monoamidation, see ref. 64, but this method was not applicable because the small amount of bisamidated side-product could not be removed from the desired mono-amidated product (amine 11).
92 C. del Pozo, A. I. Keller, T. Nagashima and D. P. Curran, *Org. Lett.*, 2007, **9**, 4167–4170.
93 This low-boiling fluorinated solvent is harmless, inflammable and miscible with almost any common organic solvent. Also, MNFB is very transparent in UV/Vis making it suitable for spectroscopic measurements. MNFB is readily commercially available as a mixture of isomers under the name HFE-7100 or Novec Engineering Fluid.
94 K. Goto, T. Miura, D. Hosaka, H. Matsumoto, M. Mizuno, H.-k. Ishida and T. Inazu, *Tetrahedron*, 2004, **60**, 8845–8854.
95 M. S. Yu, D. P. Curran and T. Nagashima, *Org. Lett.*, 2005, **7**, 3677–3680.
96 A. C. Donovan and J. F. Valliant, *J. Org. Chem.*, 2009, **74**, 8133–8138.
97 Please remember that HFIP is a toxic compound and has to be handled carefully.
98 See ESI Fig. S8.‡.
99 L. Brunsveld, J. A. J. M. Vekemans, H. M. Janssen and E. W. Meijer, *Mol. Cryst. Liq. Cryst.*, 1999, **331**, 2309–2316.
100 See ESI Fig. S1.‡.
101 K. Six, G. Verreck, J. Peeters, K. Binnemans, H. Berghmans, P. Augustijns, R. Kinget and G. Van den Mooter, *Thermochim. Acta*, 2001, **376**, 175–181.
102 See ESI Fig. S2.‡.
103 Z. Yildirim, M. Wübbenhorst, E. Mendes, S. J. Picken, I. Paraschiv, A. T. M. Marcelis, H. Zuilhof and E. J. R. Sudhölter, *J. Non-Cryst. Solids*, 2005, **351**, 2622–2628.
104 C. Destrade, P. Foucher, H. Gasparoux, N. H. Tinh, A. M. Levelut and J. Malthête, *Mol. Cryst. Liq. Cryst.*, 1984, **106**, 121–146.
105 W. Pisula, Ž. Tomović, B. El Hamaoui, M. D. Watson, T. Pakula and K. Müllen, *Adv. Funct. Mater.*, 2005, **15**, 893–904.
106 E. Fontes, P. A. Heiney and W. H. de Jeu, *Phys. Rev. Lett.*, 1988, **61**, 1202.
107 E. Fontes, P. A. Heiney, M. Ohba, J. N. Haseltine and A. B. Smith III, *Phys. Rev. A*, 1988, **37**, 1329.
108 J. Barberá, E. Cavero, M. Lehmann, J. L. Serrano, T. Sierra and J. T. Vázquez, *J. Am. Chem. Soc.*, 2003, **125**, 4527–4533.
109 W. Pisula, Ž. Tomović, C. Simpson, M. Kastler, T. Pakula and K. Müllen, *Chem. Mater.*, 2005, **17**, 4296–4303.
110 K. Nagai, K. Sakajiri, K. Maeda, K. Okoshi, T. Sato and E. Yashima, *Macromolecules*, 2006, **39**, 5371–5380.
111 J. Barberá, J. Jimenez, A. Laguna, L. Oriol, S. Pérez and J. L. Serrano, *Chem. Mater.*, 2006, **18**, 5437–5445.
112 W. Pisula, Ž. Tomović, M. D. Watson, K. Müllen, J. Kussmann, C. Ochsenfeld, T. Metzroth and J. Gauss, *J. Phys. Chem. B*, 2007, **111**, 7481–7487.
113 M. Peterca, V. Percec, M. R. Imam, P. Leowanawat, K. Morimitsu and P. A. Heiney, *J. Am. Chem. Soc.*, 2008, **130**, 14840–14852.
114 M. Lehmann, M. Jahr, F. C. Grozema, R. D. Abellon, L. D. A. Siebbeles and M. Müller, *Adv. Mater.*, 2008, **20**, 4414–4418.
115 See ESI Fig. S3.‡.
116 See ESI Fig. S4‡ for the integrated WAXS profiles.
117 See ESI Fig. S4.‡.
118 See ESI Fig. S6.‡.
119 See ESI Fig. S5.‡.
120 Such a 'quasi-hexagonal' lattice was observed for aligned films of hexabenzocoronene discotics on PTFE layers and for fluorinated hexabenzocoronenes as shown in ref. 28, 121 and 122.
121 O. Bunk, M. M. Nielsen, T. I. Solling, A. M. Van de Craats and N. Stutzmann, *J. Am. Chem. Soc.*, 2003, **125**, 2252–2258.
122 A. M. v. d. Craats, N. Stutzmann, O. Bunk, M. M. Nielsen, M. Watson, K. Müllen, H. D. Chanzy, H. Sirringhaus and R. H. Friend, *Adv. Mater.*, 2003, **15**, 495–499.
123 Discotic **1** is sparingly soluble when less than 20 vol% of HFIP is used.
124 A gCOSY spectrum for peak assignment is given in ESI Fig. S8.‡.
125 The full spectrum is given in ESI Fig. S7.‡.
126 K.-i. Tomita, A. Rich, C. d. Lozé and E. R. Blout, *J. Mol. Biol.*, 1962, **4**, 83–92.
127 Perfluorononane, unlike MNFB, is completely immiscible with any common organic solvent including chlorinated ones like chloroform.

128 J. van Gestel, A. R. A. Palmans, B. Titulaer, J. A. J. M. Vekemans and E. W. Meijer, *J. Am. Chem. Soc.*, 2005, **127**, 5490–5494.

129 L. Brunsveld, E. W. Meijer, R. B. Prince and J. S. Moore, *J. Am. Chem. Soc.*, 2001, **123**, 7978–7984.

130 All curves are given ESI Fig. S9.‡.

131 P. Toele, J. J. van Gorp and M. Glasbeek, *J. Phys. Chem. A*, 2005, **109**, 10479–10487.

132 The boiling point of NMFB is 61 °C and that of perfluorononane 125 °C.

133 The extinction coefficients of the mixtures are stable in time.

134 All curves are given in ESI Fig. S10.‡.

135 Concentration dependent spectra of disc **2** in F1 : 10 are given in ESI Fig. S11.‡.

136 See ESI Fig. S11.‡.

137 The annealing step is necessary to reach the thermodynamically most stable state; the optical spectra of the non-annealed mixture change slowly in time to reach a final state while the optical spectra of the annealed mixtures are stable in time at this final state.

138 Chiral, C_3-symmetrical disc **2** has to be mixed with at least 10 mol% of fluorinated disc **1** to achieve complete dissolution.

139 Please note that the maxima in the CD spectra do not display a red or blue shift.

140 Full CD and absorption spectra are given in ESI Fig. S12 and S13.‡.

141 Full CD and absorption spectra are given in ESI Fig. S14 and S15.‡.

142 M. Yano, T. Taketsugu, K. Hori, H. Okamoto and S. Takenaka, *Chem.–Eur. J.*, 2004, **10**, 3991–3999.

143 K. Hori, M. Maeda, M. Yano and M. Kunugi, *Liq. Cryst.*, 2011, **38**, 287–293.

144 J. J. Van Gorp, *Helices by hydrogen bonding: folding and stacking of chiral supramolecular scaffolds*, PhD thesis, Eindhoven University of Technology, 2004.

145 In the solid state, fluorinated disc **1** and hydrocarbon discs **2** or **3** do not co-exist in common aggregates as only phase transitions belonging to the pure compounds were detected by DSC and polarizing optical microscopy.